Experimental verification of the greenhouse effect

2. Communication: The background radiation of clouds and aerosols

Abstract

The greenhouse effect of the most important atmospheric IR gases was investigated with a new type of apparatus in the so-called "cooling mode. Only with this type of test implementation can the mutual influence of the radiation of the greenhouse gases and the background radiation of the aerosol plate study. The relationships found in the laboratory are relevant for climate research, since the same laws have been proven in nature as well. Nature observations by Ångström and many other meteorologists and climate researchers led to the realization that the atmospheric counterradiation depends on the air temperature and humidity, but especially on the background radiation of the clouds. The laboratory and field experiments consistently show that greenhouse gases and clouds/aerosols are radiation competitors, which hinder each other in the near-Earth greenhouse effect and significantly reduce the effectiveness of each other. A knowledge of our ancestors, which has obviously been lost, is revealed.

1. Introduction

In the first communication /1/, a novel apparatus was presented, which, in contrast to the previously known methods of investigation, does not investigate the emitted IR radiation (transmission) but the IR counterradiation (greenhouse effect) of IR-active gases. The apparatus contains as essential components a so-called earth plate and at a large distance an aerosol plate, which are representative of the earth's surface and a cloud layer. In a first test with propane as a model greenhouse gas, it was found that this gas can increase an already existing, construction-related background radiation E_B under certain conditions. This study was repeated with methane, CO2, nitrous oxide, butane, and Freon 134a. For this purpose, the tempered at 16 ° C apparatus was filled with 1.3% by volume of the IR gas and then only the aerosol plate gradually cooled to - 18 ° C. At each cooling step, the electric heating Q_E was determined, which is required for a constant temperature of the earth plate of 16.09 ° C (for experimental data see chapter 4).

This type of test implementation is called "cooling mode" because the temperature of the aerosol plate is gradually reduced. This technique can be used to examine the interaction of an IR-gas radiation with the background radiation of the aerosol plate. In the alternative experimental procedure, the "concentration mode", the radiations of the IR gases are analysed at constant temperatures but different concentrations of the gases. Here, from the outset, the aerosol plate is much colder than its surroundings. This method is more suitable to determine the concentration-dependent emissivities of the IR gases, which is to be reported in the following messages.

The electric heating Q_E are plotted against the temperature of the aerosol plate T_B (as $T^4/10^8$, in Kelvin) in an Excel diagram (Fig. 1). The second X-axis Tp_B in °C serves for orientation. For the sake of clarity, the individual measuring points from +16 to -18 ° C are only indicated for Freon.

In the first communication /1/ it was derived that the heating of the earth plate Q_E is numerically identical to the radiative cooling P_E. The radiative cooling P_E is the energy that the earth plate would lose as the difference of its IR transmission M_E and receiving an IR-counterradiation E_B (equation 1). In this equation, M_E is the IR emission of the earth plate of 396.9 W/m^2 (calculated according to Stefan-Boltzmann, ε = 1).

In order to prevent cooling of the earth plate by radiation cooling, heat must be supplied to it from the outside. The earth plate has a constant temperature if $Q_E = P_E$. The y-axis therefore also shows the radiation cooling P_E, which is influenced by the IR-gases.

Equation 1: Radiation cooling P_E: $P_E = M_E - E_C$

It is possible to characterise the greenhouse effect with the radiation cooling P_E or with the counterradiation E_C, since both variables are linked together as indicated in equation 1. But beware! Radiation cooling and counter-radiation behave in opposite directions. A strong counterradiation results in low radiation cooling!

In the literature, the radiation cooling (equation 1) is known as the "effective radiation" of the Earth. The alternative term "radiation cooling" shows that this is a cooling by IR radiation. This is to emphasize that the earth has other cooling possibilities, such as Water evaporation or convection.

From the experimentally determined measuring points, the linear Excel trend lines are calculated (tab 1). The trend lines consist of a constant part P_E (T_B = 0) (maximum radiation cooling without counterradiation from the aerosol plate) and a variable part dP_E / dT_B (course of the straight line).

All newly investigated IR-active gases show a similar radiation behavior as propane, but with significantly different radiation cooling P_E. Thus, the very simple experimental apparatus proves to be quite suitable to check the near-Earth greenhouse effect. The IR gases are arranged in tab 1 according to the effectiveness of their greenhouse effect (reduction of radiation cooling P_E). A first surprise is the order of methane and CO2. Methane, supposedly a much stronger greenhouse gas than CO2, proves to be the weaker IR emitter here. Since the current series of experiments focused on the influence of background radiation, the unexpected result of methane radiation should not be commented on here.

In another series of tests (but then in concentration mode) all the above-mentioned IR-gases were examined again in terms of their radiation capability. The lower IR radiation of methane was once again detected in comparison to CO2, which is to be reported later.

Table 1: Excel trend lines for the radiation cooling of the earth plate: $P_E = dP_E/dT_B \cdot T_B + P_E(T_B{=}0)$

IR gas	$P_E(T_B{=}0)$	dP_E/dT_B	R^2
without	294,9	-4,232	0,9997
Methane	281,5	-4,074	0,9991
CO2	279,3	-4,041	0,9984
Nitrous oxide	272,6	-3,945	0,9988
Propane	267,4	-3,876	0,9994
Freon 134a	174,9	-2,553	0,9987

$P_E(T_B{=}0)$: radiation cooling without radiation of the aerosol plate, dP_E/dT_B: increase of the trend lines, R^2: specification of the linearity, T_B = temperature of the aerosol plate in Kelvin as $T^4/10^8$

The measurement in the cooling mode makes it possible to represent the mutual influence of the IR gas radiation and a background radiation in a single diagram. The aerosol plate is referred to as a background emitter, since it is located behind the IR gases from the perspective of the earth plate. The aerosol plate seems to be of little importance for the greenhouse effect, since most of its radiation is obscured by the IR gases and thus acts only in the background. This is a fundamentally wrong assessment, as shown below.

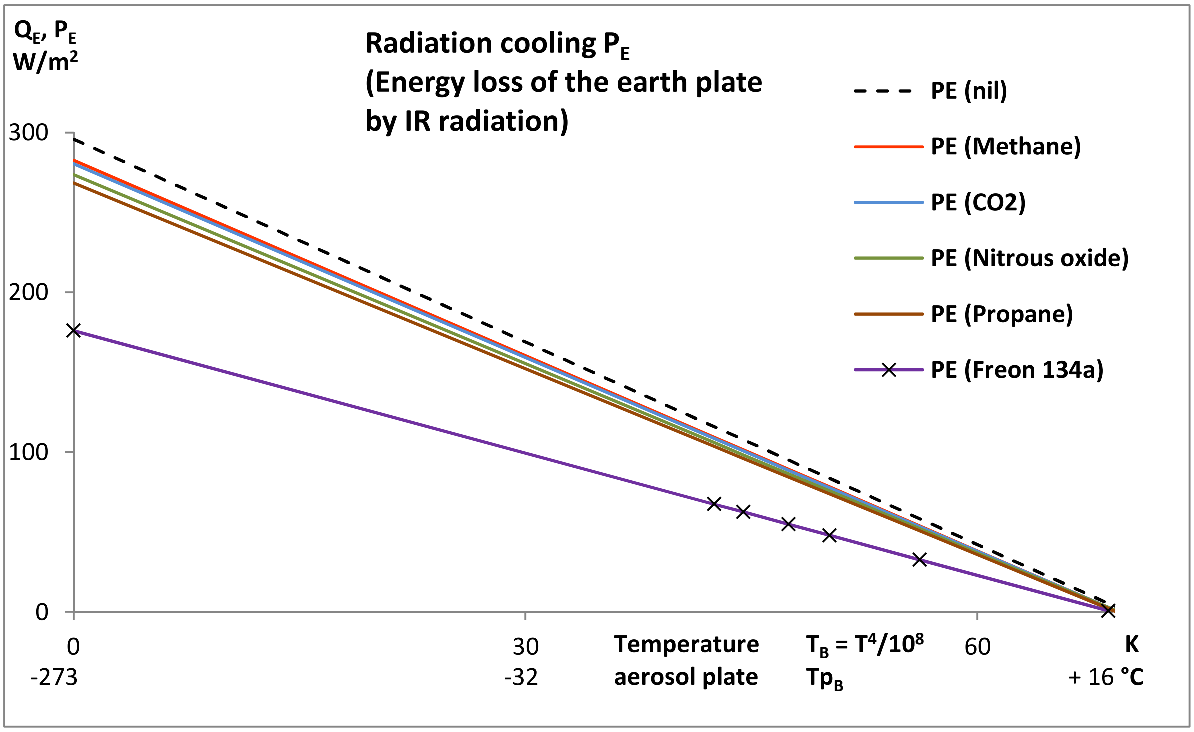

Fig. 1: Influence of the radiation cooling of the earth plate P_E by IR gases and by the temperature T_B of the aerosol plate

From Fig. 1 it can be seen that the radiation cooling of the earth plate P_E is not only dependent on the effectiveness of an IR gas, but also on the temperature of the aerosol plate T_B.

The greater the radiation capacity of an IR gas, the lower the energy loss of the earth plate by IR radiation (radiation cooling P_E). On the other hand, the radiation cooling P_E is also influenced by the temperature of the aerosol plate, as can be seen on the sloping (negative) course of the trend lines. The effect of IR gases can even be zero if earth and aerosol plate have the same temperature. This relativization of the greenhouse effect by a background radiation was derived in detail in the first communication.

The reduction of the greenhouse effect is caused by a kind of countermovement. When the radiation of a greenhouse gas E_F (as a foreground emitter) increases (decreases), it also reduces (increases) to some extent the part of the background E_B (T_B) that actually reaches the Earth plate (equation 2). Ultimately, by this countermovement, the increase (decrease) of the collective counterradiation of both radiation sources (E_C) is always smaller than the sum of the theoretical radiation of foreground and background. Foreground and background emitters may be referred to as radiation competitors, which hinder each other during the IR irradiation of the Earth's surface E_C /1/.

Equation 2: Counter radiation of the near-Earth atmosphere E_G: $E_C = E_F + E_B(T_B)$

This relationship is of fundamental importance and also applies to clouds. On the one hand, clouds can reflect up to 90% of the sun's rays depending on the thickness and type of clouds (cloud albedo, /2/) and thus cool the earth. On the other hand, clouds as IR emitters also cause warming of the earth, which has made their assessment so difficult so far. The competition with greenhouse gases reduces only the contribution of the clouds to the IR-irradiation of the Earth (its warming side) and not the cloud-caused scattering and reflection of the sunlight. Because of this one-sided influence of greenhouse gases, a reassessment of clouds should be required. It can be assumed that, contrary to the doctrine, any form of clouds contributes to the cooling of the Earth! So far the teaching was that only deep, optically dense clouds cool the earth, but high, optically thin clouds warm the earth /3/.

The mutual competition means that conversely clouds/aerosols reduce the effectiveness of the greenhouse gases. Therefore, doubts about the IPCC formula for the CO2-radiation force are appropriate (equation 3), because only the theoretical CO_2 emission is calculated without background radiation. A detailed discussion of this IPCC formula and the presentation of a CO_2 radiation formula will be given in the next communication.

Equation 3: CO2 Radiation Force (IPCC $dF = 5{,}35 \cdot \ln(C/C_0)$ W/m^2

From Fig. 1 it can also be seen that a measurement of the IR gas radiation (with this apparatus) is possible only against a much colder background. When the earth and aerosol plates are at the same temperature, the radiation cooling P_E is zero, regardless of whether greenhouse gases are present or not.

In addition, greenhouse gases (at certain wavelengths) are transparent. The IR sensor (the earth plate) "sees" not only the IR gases, but also the background (aerosol plate). Both sources of radiation thus enter the IR measurement. Ideal would be a background with the temperature $T_B = 0$, with no IR radiation. The high linearity R^2 (Pearson function> 0.998) of the found trend lines PE (Table 1) during cooling down to -18 ° C makes it possible, however, to calculate by extrapolation up to $T_B = 0$. Thus, the pure IR gas radiation (their theoretical radiation potential), without background radiation of the aerosol plate, can be determined.
In addition to the radiation of the aerosol plate, there is still a radiation of the aluminium wall of the apparatus, which as a constant affects the measurements and was determined in the measurement "nil" with 102 W/m^2 /1/.

The experiments presented are only laboratory studies that model the greenhouse effect of the near-Earth atmosphere. But is the IR radiation of the real atmosphere also influenced by clouds? This is a question that the pioneers of climate research have already made. As early as the beginning of the 20th century, Knut Ångström developed a Pyrgeometer that could detect the "dark" (IR) radiation of the atmosphere /4/. As with the presented apparatus, the electrical current was measured which is required for a constant temperature of a blackened, thermocouple exposed to the sky. In this way, the presented, own apparatus is a reference to the Pyrgeometer by Knut Ångström. His son, Anders Ångström, and Sten Asklöf studied the nocturnal "heat radiation" in different regions of the earth and found that it depends on the air temperature and the humidity but above all on the degree of cloud cover /5/. It has been found that the effective radiation (radiation cooling) of the earth with cloudy sky is only about 23% compared to the clear sky. These first, simple measurements of the Earth's effective IR radiation were checked by later measurements with improved equipment. It was found that: "*When the sky was overcast, the intensity of the effective radiation averaged 18.5% of the value in a cloudless sky*" /6/.

The fact that clouds, as powerful IR emitters, can considerably reduce the cooling down during the night (for example in winter) has become common knowledge in the meantime. Due to the many well-known investigations, own measurements would not have been necessary. In the meantime, however, the devices for measuring the IR radiation thanks to microelectronics not only much more handy, but above all have become more affordable. In order to learn the atmospheric counterradiation with own eyes, the IR radiation of the sky over Berlin was measured from July 2016 to May 2017 at irregular intervals with a pyrometer PCE-891 (an infrared thermometer) at different degrees of cloudiness. As expected, the cloudy sky measurements showed a very strong counterradiation caused by clouds. Unexpectedly exciting were the measurements of the cloud-free sky. According to F. Möller, only the IR gases water vapor, CO_2 and to a lesser extent ozone, methane and nitrous oxide are the cause of the clear sky atmospheric radiation, which can be calculated with his radiation diagrams /7/. The IR radiation of water vapor and CO_2 is not disputed. In the following chapters, however, it is shown that the non-visible aerosols are highly likely to generate significant IR radiation and that a rethink is required here.

2. The cloud-free sky – the radiation of invisible aerosols?

According to Wikipedia, the IR-active gases are the only IR emitters that send a counterradiation to the earth in clear skies. *„When the sky is clear, the reflected radiation consists mainly of the heat radiation of the atmosphere gases "* /8/.

Thus, with a Pyrgeometer (in the IR wavelength range of 5 to 25 µm) from a weather station near Munich on October 6, 2005, the course of the counter-radiation during one day was measured: *"During the morning high fog prevailed. The fog droplets contributed as efficient long-wave radiators to relatively high radiation values of approx. 370 W/m². Around noon, the fog dissolved and left behind a clear sky. The atmospheric gases alone are less efficient long-wave emitters, so the radiation levels dropped noticeably to about 300 W/m². ... averaged over the year and across the globe, the intensity of the counter radiation is about 300 W/m² "*.

The thesis of an exclusive IR gas radiation coincides with the statement of modern meteorologists: "The clear sky contains only a few smallest particles. There is a pure gaseous atmosphere and no aerosol ... "/9/.

The hypotheses, however, provoke doubts, because then the large metropolitan areas of the earth would not have a fine dust problem, there would be no Sahara dust, the plants would come out without pollen and it would be questionable how clouds can form at all, because: *"The water droplets (the Clouds) are formed around condensation cores (aerosols) when the relative humidity of the air exceeds 100% (by at most 1%)*" /10/.

In fact, there are a number of observations and circumstantial evidence, all of which point out that the atmospheric counterradiation in cloud-free skies is jointly generated by IR-active gases (mainly water vapor and CO2) and the non-visible aerosols. Three completely different studies are performed: Own temperature measurements of the clear sky over Berlin (chapter 2.1), measurements of the ground temperature from a higher altitude (chapter 2.2) and calculations of water vapor radiation with formula of Ångström and other researchers (chapter 2.3). Each of these arguments may be questionable on its own, but in their sum they form a conclusive concept of an aerosol radiation, which has obviously been neglected by modern climate research. The forefathers of meteorology initially agreed that: *"Millions of dusts particles are in the air and even make a contribution to the so-called return or cold convection during the nocturnal cooling"* /11/.

2.1. Temperature measurements of the cloud-free sky

For the exploration of atmospheric radiation, the cloud-free sky over Berlin was scanned at different day and night times with a Pyrometer PCE-891 (an infrared thermometer). The Pyrometer used has a built-in filter that only allows IR rays of the wavelengths 8-14 µm and is equipped with an optic 50:1, which allows a focus. This means that the pyrometer measures in a wavelength range that is only slightly affected by CO2 or water vapor (atmospheric window). The temperature of the sky was recorded at elevation angles from 0 to 90 degrees (angle above the horizon). The measurement at 0 degrees was equated with the air temperature at a height of 1.8 m. The measured values found are extremely dependent on the elevation angle (Tab. 2). On average, a difference of 22 K was found between the angle measurements of 20 and 90 degrees. The strong angular dependence can be explained by weak IR emitters, which require a large layer thickness (several kilometres) for the saturation of their radiations. In the vertical measurement, the proportion of the cold atmospheric layers is greater than at the flat 20 degrees angle. In order to get an idea of what the temperature measurements mean, a "radiation equivalent" was specified in the table in W/m^2. It is the radiation density that a "black body" would emit at the measured temperatures.

Who or what causes these IR radiations? The measuring range of the pyrometer of 8 - 14 µm is too large to exclude greenhouse gases per se. First there is the ozone, which has an emission maximum at 9.6 µm, that is, quite in the middle. The ozone emissions are very small, even in the centre not saturated bands that can be neglected. From the measurements of the weather satellite Tiros in the wavelength range 7.5 - 13.5 µm, it is known that CO2 and water vapor also emit IR emissions in this wave range to a small extent (see chapter 2.2). So these two greenhouse gases can partly explain the angular dependence. However, the observed differences in the sky radiation of 90 W/m^2 between the 20 and 90 degrees measurement (Table 2, B - D) are too high to be explained by H2O and CO2 radiation alone. Finally, these gases do not have a major peak in the wave range of the pyrometer, but only extensions that affect the measurement as tailpipes. Thus, the only plausible explanation is the assumption of a common radiation of greenhouse gases and aerosols. Aerosols, as solid or liquid particles, produce a continuous radiation with a maximum between 11 and 12 µm (Wien's law of displacement), which coincides perfectly with the measuring range of the pyrometer.

Table 2: Clear Sky Temperature Measurement: Pyrometer PCE-891

		Elevation angle				Temperature-differences in K	
		A: 0°	B: 20°	C: 45°	D: 90°		
Date	Time	Temperatures °C				A - D	B - D
19.07.2016	22:00	16,06	4,14	-11,14	-15,92	32,0	20,1
21.07.2016	18:45	27,42	7,34	-7,86	-14,32	41,7	21,7
18.08.2016	19:20	21,7	6,2	-13,7	-21,7	43,4	27,9
24.08.2016	21:30	18,7	7,5	-12,3	-23,1	41,8	30,6
30.08.2016	19:45	18,7	0,4	-21,2	-28,5	47,2	28,9
08.09.2016	19:20	23,1	5,1	-14,8	-23,4	46,5	28,5
15.09.2016	07:00	15,5	0,8	-17,7	-27,8	43,3	28,6
12.09.2016	06:30	14,6	-10,4	-13,8	-16,2	30,8	5,8
15.09.2016	07:00	15,5	0,8	-17,7	-27,8	43,3	28,6
28.01.2017	16:40	3	-22	-30,5	-33,1	36,1	11,1
13.02.2017	08:50	-2,5	-21	-31	-32,8	30,3	11,8
17.05.2017	22:15	19,7	5,5	-12,3	-20	39,7	25,5
Average °C		16,0	-1,3	-17,0	-23,7	**39,7**	**22,4**
Radiation equivalent W/m^2		396	310	244	220	176	90

A: Air temperature at a height of 1.80 m.

The angular dependence of the IR counterradiation in clear skies is by no means a new discovery. As early as 1933, on the night of May 19 to 20, in Föhren near Trier, an "effective actinometer" revealed a dependency of the effective radiation (radiation cooling) on the elevation angle (Table 3) /12/.

Table 3: "Meridional intensity distribution of effective radiation in relative units, zenith = 100" according to Kessler and Kaempfert

Height above horizon in degrees	0	10	20	30	40	50	60	70	80	90
Intensity in hundredths	0	23	43	58	70	79	86	92	96	100

2.2. Temperature measurement of the Earth's surface from a higher height

In July 1961 the weather satellite TIROS III was brought into orbit by NASA, which was equipped with an IR sensor (TIROS Channel 2, IR sensitivity range of 7.5 – 13.5 µm). It turned out that the radiation temperatures measured in orbit are always lower than the actual temperatures on the ground. It was recognized that the temperature measurements were influenced by the (cold) atmosphere. The "Atmospheric window" in the range 7.5 – 13.5 µm was obviously not as transparent as hoped. In particular, the IR radiations of water vapor, CO2 and ozone were identified as the cause of this atmospheric radiation. Strangely enough, the non-visible aerosols as a further radiation source were ignored. But there was a clear indication of possible aerosol radiation. The deviation was 13.3 K in an "extremely humid" atmosphere over Panama (15.11.1961). Over the dry Sahara desert (Colomb-Bechar, 15.07.1961) the deviation was still 8.8 K despite low water concentration /13/. This is a value that provides enough space for aerosol radiation.

Another reference can be found in the report on temperature measurements of water surfaces from a height of up to 2400 m (from aircraft or helicopters) with a PRT radiometer in the spectral range 8 - 13 µm. As with the measurements of the Tiros satellite, a deviation between the radiation temperature and the actual surface temperature was detected. Due to the lower height, the deviation was correspondingly smaller with 2 - 3 K. The influence of the air humidity proved to be less than expected: *"Experience shows that the humidity has a much lower influence on the correction values for the radiation temperature than the air temperature"* (14). Even if the author does not mention the role of aerosols, his observed deviations can be interpreted as aerosol radiation.

2.3. The water vapor radiation in cloudless sky

The measurements of the cloud-free sky with the Ångström Pyrgeometer showed that the atmospheric counter-radiation depends on the temperature and humidity of the air. Ångström was guided by the consideration that the effective IR radiation A_e of the earth is formed by the difference between its radiation ($\sigma \cdot T^4$) and the counter-radiation of the atmosphere (G) (Equation 4, see also Equation 1) /5/. By reversing the equation, the counter-radiation G is the difference between earth and effective radiation. According to Ångström, the effective emittance A_e is calculated by a modified Stefan-Boltzmann equation whose coefficients were determined experimentally. Assuming that near-Earth atmosphere and Earth's surface have the same temperature, the counterradiation G can be calculated according to Equation 4.

Equation 4: Ångström formula

Counter radiation G in cloudless sky:

$$A_e = \sigma \cdot T^4_{Earth} - G$$

$$G = \sigma \cdot T^4_{Earth} - A_e$$

$$A_e = T^4_{Air} \cdot (0.194+0.236 \cdot 10^{-0.069 \cdot e})$$

$$G = \sigma \cdot T^4_{Air} \cdot [1-(0.194+0.236 \cdot 10^{-0.069 \cdot e})]$$

e = Water vapor partial pressure at the station, in mm Hg

T_{Air} = Station temperature (2 m height, in K)

Extensive measurements in subsequent years confirmed that the counterradiation depends on air temperature and humidity. The coefficients were corrected by Bolz and Falkenberg /15/.

Equation 5: Bolz / Falkenberg formula

$$G = \sigma \cdot T^4_{Air} \cdot (0.82-0.25 \cdot 10^{-0,12 \cdot e})$$

In climate research, it is now common to use radiation diagrams to calculate atmospheric emission and counter-radiation based on the absorption lines of the IR-active gases /7/. The calculations require mainframes and are difficult for an outsider to understand and above all not verifiable. Since the results of Ångström were confirmed in principle, the water vapor radiation can be further calculated with the simple or corrected Ångström formula. Above all, the calculations are trustworthy because they have been confirmed by a large number of field trials. Table 4 shows the atmospheric counterradiation at an air temperature of 15 ° C, calculated according to the formula of Bolz/Falkenberg for air humidity from 0 to 100% (values in brackets were calculated according to the Ångström formula). The fraction of the water vapor radiation on the calculated counterradiation was determined from the increase of the radiation to the base value of 223 W/m^2 (without water vapor, relative humidity = 0).

The calculations reveal two fundamental contradictions: In a clear sky at 15 ° C the atmospheric counterradiation is only caused to a small extent (30% according to Bolz/Falkenberg) by water vapor, and the H2O radiation is much smaller than would be expected after the absorption bands of the water vapor.

The above mentioned thesis: "*When the sky is clear, the reflected radiation consists mainly of the heat radiation of the atmosphere gases*" is **not confirmed** by these calculations. If the CO2 radiation (supposedly around half of the H2O radiation) is added to the water vapor radiation, the most important IR active gases only account for around 45% of the atmospheric counter radiation. 55% of the atmospheric radiation is thus not generated by greenhouse gases! There must be an additional source of radiation (the radiation of the aerosols?) to explain the measured counterradiation of the sky.

Table 4: Calculations of the atmospheric counter-radiation in a clear sky at 15 ° C after Bolz/Falkenberg and Ångström (in brackets)

relative Humidity %	e_{H2O} *) mm Hg	Calculated Counterradiation W/m2	H2O Radiation W/m²	Proportion of H2O Radiation %
100	12,78	318 (303)	95 (80)	30 (26)
80	10,23	315 (297)	92 (74)	29 (25)
60	7,67	309 (288)	86 (65)	28 (23)
40	5,11	297 (274)	74 (51)	25 (19)
20	2,56	272 (254)	50 (31)	18 (12)
0	0,00	223 (223)	0 (0)	0 (0)

*) Humidity and pressure converter - Cactus2000

But also the maximum achievable H2O radiation of 95 W/m² at 100% relative humidity is amazing. This value is only 50% of the theoretical H2O radiation of around 190 W/m². The latter is an estimate derived from Planck's Law of Radiation and the assumption of saturation of all H2O-typical absorption bands between 5 - 8 and 17 - 100 µm at 15 ° C.

These contradictions can be dissolved by a common counter-radiation of water vapor and aerosols, which in chapter 3 will be discussed in more detail.

Note: The Ångström Pyrgeometer has no radiation filter. All relevant wavelengths of the atmospheric counterradiation are recorded. Thus, unlike in the own measurements (chapter 2.1), the total atmospheric counterradiation is measured here.

3. The IR counterradiation under clouds

3.1. Temperature measurements of the overcast sky

By the same method as in chapter 2.1 described, the cloud-covered sky (deep layer clouds) over Berlin was scanned with the Pyrometer PCE-891 (Table 5).

As already stated in the temperature measurement in clear skies, the measurements capture only part of the atmospheric counterradiation (wavelength range of 8-14 µm). The large increase in IR radiation of 122 W/m² (90 degree measurements), compared to the cloudless sky (Tab. 2 and Tab. 5), clearly shows that the radiation of the clouds is mainly measured here.

Otherwise, this series of measurements under clouds is characterized by a lower angular dependence of the measured values of 3.3 K between the 20 and 90 degree measurement resulting from the relatively short distance between ground and clouds. This confirms the hypothesis that the angular dependence of the temperature measurements is caused by weak emitters of the atmosphere, which require several kilometres of atmosphere for a saturated radiation, which is only partially available under clouds.

Table 5: Temperature measurement of the covered sky: Pyrometer PCE-891

		Elevation angle				Temperature-differences in K	
		A: 0°	B: 20°	C: 45°	D: 90°		
Date	Time	Temperatures °C				A - D	B - D
19.07.2016	07:00	18,8	17,2	16,4	14,3	4,6	3,0
12.08.2016	18:10	19,9	16,5	14,8	14,5	5,4	2,0
19.08.2016	09:25	20,0	16,1	11,9	10,2	9,8	5,9
29.01.2017	17:00	7,8	0,1	-1,7	-3,4	11,2	3,5
07.02.2017	16:30	3,1	0,7	-1,5	-1,7	4,8	2,4
09.05.2017	06:30	7,0	1,5	-1,3	-2,9	9,9	4,4
24.05.2017	12:00	15,5	9,5	8,0	7,5	8,0	2,0
Average °C		13,2	8,8	6,7	5,5	**7,7**	**3,3**
Radiation equivalent W/m²		381	358	348	342	39	16

A: Air temperature at a height of 1.80 m.

3.2. The water vapor radiation of the overcast sky

In agreement, Ångström and Asklöf found that the effective radiation A_W of the earth in the presence of clouds is significantly reduced depending on the degree of cloud cover and its height. A_W is obtained from the effective radiation A_0 (clear sky) by multiplying by the coefficients k and w /5/.

Equation 6: **Ångström / Asklöf formula:** $A_W = A_0 \cdot (1 - k \cdot w/10)$
k = 0.8 - 0.9 (low clouds), 0.7 and 0.2 (medium and high clouds), kØ = 0.765, w = cloud coverage

The counterradiation for the completely covered sky (w = 10) and an average cloud height (k = 0.765) is given by Equation 7, where for A_0 the expression A_e from Equation 4 is used.

Equation 7: Counter Radiation in Cloudy Sky: $G = \sigma \cdot T^4_{Air} \cdot [1-(0{,}194+0{,}236 \cdot 10^{-0{,}069 \cdot e}) \cdot (1- 0{,}765)]$

Tab. 6 shows the atmospheric counterradiation with complete cloud coverage and an air temperature of 15 ° C, at relative humidity from 0 to 100%. The proportion of water vapor radiation in the calculated counterradiation was determined from the increase of the IR radiation to the base value of 351 W/m² (without water vapor, relative humidity = 0).

Table 6: Atmospheric counter-radiation calculations at full cloud coverage and 15 ° C to Ångström / Asklöf

relative Humidity %	e_{H2O} *) mm Hg	Calculated Counterradiation W/m2	H2O Radiation W/m²	Proportion of H2O Radiation %
100	12,78	370	19	5,1
80	10,23	369	17	4,7
60	7,67	367	15	4,2
40	5,11	363	12	3,3
20	2,56	359	7	2,0
0	0,00	351	0	0,0

*) Humidity and pressure converter - Cactus2000

The first thing to notice is the low impact of air humidity. Even at 100% relative humidity, the proportion of the water vapor radiation is only 5% (19 W/m^2) of the calculated counter-radiation of 370 W/m^2.

Due to the low effect of the water vapor, alternative formulas were proposed by other researchers, which omit the water vapour completely ("since it goes down in the measuring accuracy") and only consider the cloud cover as a parameter /15/.

As a reminder, the counterradiation (near-Earth greenhouse effect) has an immediate and direct effect on the cooling (radiation cooling) of the earth according to Equation 1. At 15 ° C (100% humidity), the earth can only get rid of 21 W/m^2 (391 - 370) by IR radiation. No wonder that the temperatures barely decrease during a night's cooling under a closed cloud cover. But the key point is that water vapor accounts for only 5% of this strong effect. This realization is particularly important given the current global warming debate. Water vapor is not any greenhouse gas, but the most active IR-active gas in the atmosphere, which is said to account for 66 to 85% of all absorbed IR radiation /16/.

The nature observations (formulas) of the early researchers confirm in full the own laboratory tests and conclusions derived therefrom. After that, the greenhouse gases in the presence of a closed cloud cover almost completely lose their efficacy.

Even modern IR spectroscopic measurements of atmospheric counterradiation in Barrow, Alaska, show that the near-Earth greenhouse effect of IR-active gases can completely disappear under clouds /17/.

Also a comparison of the two radiation calculations (Tab. 4 and Tab. 6) for the clear and cloudy sky offers some interesting aspects:
Without water vapor (relative humidity = 0), clouds cause an increase in counterradiation of 128 W/m^2 (351 vs. 223 W/m^2). *A comparable value of 122 W/m^2 was found for the own temperature measurements, but in the measuring range 8 - 14 µm (chapter 3.1).*

But in a humid atmosphere (100% relative humidity) the cloud-induced increase is only 67 W/m^2 (based on Ångström values 370 vs. 303 W/m^2) (Table 4 vs. Table 6).

These considerations are further proof that with a common radiation of greenhouse gases and clouds both radiation sources lose their effectiveness. The correlations found in the laboratory are thus by no means new, but only show experimentally, what was originally the teaching opinion and firm knowledge of meteorologists and climate researchers.

Modern climatology has replaced the earlier near-Earth counter-radiation determinations by spectroscopic IR (transmission) measurements at the top of the atmosphere (TOA) from the perspective of weather satellites (e.g., Nimbus 4). The TOA spectra show distinct absorption cones for ozone but above all for CO2, which contribute to a reduction of the total transmission. It is concluded that the Earth must heat up to compensate for the missing transmissions with the other wavelengths. This interpretation assumes that there are no other emitters between TOA and Earth's surface. But if one accepts the existence of the aerosols and clouds as further emitters of the atmosphere, one can conclude that not directly the Earth's surface, but the aerosols and the tops of the clouds warm up a bit. A process that should indirectly affect the temperature of the Earth's surface, but much weaker than the directly effective IR back radiation of the near-Earth greenhouse effect.

The IR radiations of the clouds and aerosols are similar radiation components of the atmosphere with continuous transitions. Aerosols and water droplets are characterized by a very large surface (in terms of their mass). This is an important prerequisite for surface radiation of solid and liquid substances. In the atmosphere, this particle radiation depends on its concentration (particles per m^3 of air) and the temperature of its surroundings, as can be clearly seen in Fig. 2.

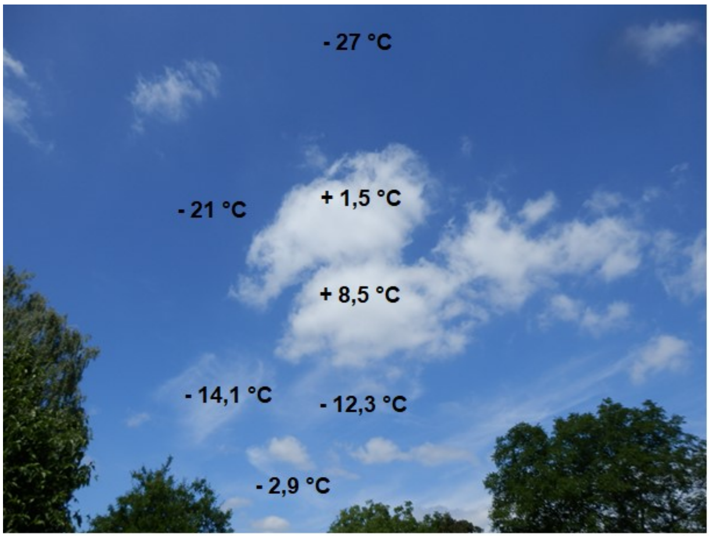

Fig. 2: Berlin on 14.06.2017, 12:20, air: 20.0 °C (1.8 m): temperature measurements of different density clouds and cloud-free sections.

4. Appendix- Experimental data

Q_E is the electrical heating of a fictitious earth plate with an area of 1 m^2. The actually measured values of the earth plate used (219.04 cm^2) are smaller by a factor of 0.0219. U_B is the voltage of 5 series-connected Peltier elements (TEC1-12706) on the aerosol plate measured with the Voltmeter (Voltacraft VC 250). These elements register the IR radiation (earth plate, sidewall and IR gas emissions) and the heat conduction of the immediate environment. Since the heat conduction during cooling of the aerosol plate is constantly increasing, U_B is not evaluated in experiments in the cooling mode, but is only indicated for information in the following tables.

Nr. 145: ohne IR-Gase			dQ_E/dT_B = -4,232; $Q_E(T_B$=0) = 294,9				
Tp_E °C	Tp_B °C	Tp_1 °C	Tp_2 °C	Tp_3 °C	Tp_4 °C	Q_E W/m^2	U_B mV
16,09	15,89	15,90	15,90	15,85	15,70	0,13	-0,25
16,09	1,08	15,55	15,55	15,50	15,10	55,01	47,80
16,09	-5,83	15,50	15,40	15,40	14,80	77,83	69,55
16,09	-9,99	15,40	15,30	15,20	14,70	91,75	81,60
16,09	-15,03	15,25	15,20	15,10	14,50	107,02	95,75
16,09	-19,58	15,20	15,10	15,05	14,30	120,88	108,25

Ø von Nr. 208 + 209: 1,3 % Methan			dQ_E/dT_B = -4,074; $Q_E(T_B$=0) = 281,5				
Tp_E °C	Tp_B °C	Tp_1 °C	Tp_2 °C	Tp_3 °C	Tp_4 °C	Q_E W/m^2	U_B mV
16,09	15,49	16,03	16,08	16,08	16,30	0,00	0,91
16,09	5,60	15,85	15,78	15,83	15,80	35,07	36,33
16,09	-0,37	15,65	15,70	15,65	15,63	54,99	58,38
16,09	-6,74	15,58	15,63	15,58	15,43	74,67	78,98
16,09	-10,50	15,50	15,60	15,48	15,30	87,45	90,60
16,09	-14,45	15,45	15,53	15,40	15,28	99,53	102,98
16,09	-17,49	15,43	15,40	15,30	15,10	109,01	112,95

Ø von Nr. 206 + 207: 1,3 % CO2			dQ_E/dT_B = -4,041; $Q_E(T_B=0)$ = 279,3				
Tp_E °C	Tp_B °C	Tp_1 °C	Tp_2 °C	Tp_3 °C	Tp_4 °C	Q_E W/m²	U_B mV
16,09	15,7025	16,025	16,025	16,075	16,2	0	0,85
16,0875	6,06	15,875	15,8	15,825	15,75	32,75	35,28
16,09	-0,015	15,65	15,7	15,675	15,55	52,18	57,55
16,09	-6,145	15,575	15,6	15,5	15,225	72,75	76,65
16,09	-10,315	15,5	15,525	15,375	15,1	86,36	89,45
16,09	-14,265	15,475	15,475	15,35	14,975	98,73	102,78
16,09	-17,47	15,475	15,375	15,3	14,9	108,12	113,40

Ø von Nr. 210 + 211: 1,3 % Lachgas			dQ_E/dT_B = -3,945; $Q_E(T_B=0)$ = 272,6				
Tp_E °C	Tp_B °C	Tp_1 °C	Tp_2 °C	Tp_3 °C	Tp_4 °C	Q_E W/m²	U_B mV
16,09	15,52	16,03	16,10	16,10	16,28	0,00	1,21
16,09	5,78	15,80	15,83	15,80	15,75	33,64	36,10
16,09	-0,51	15,70	15,73	15,70	15,55	52,83	58,78
16,09	-6,90	15,58	15,63	15,48	15,25	72,70	79,85
16,09	-10,77	15,50	15,58	15,40	15,18	85,52	91,58
16,09	-14,96	15,43	15,48	15,30	15,08	98,15	104,78
16,09	-17,83	15,40	15,40	15,30	14,98	106,30	114,10

Nr. 212: 1,3 % Propan			dQ_E/dT_B = -3,876; $Q_E(T_B=0)$ = 267,4				
Tp_E °C	Tp_B °C	Tp_1 °C	Tp_2 °C	Tp_3 °C	Tp_4 °C	Q_E W/m²	U_B mV
16,09	15,20	16,10	16,10	16,10	16,50	0,00	2,90
16,09	7,06	15,90	15,85	15,85	15,80	28,87	32,50
16,09	-0,36	15,70	15,75	15,60	15,50	51,68	58,90
16,09	-7,41	15,60	15,65	15,40	15,20	72,75	82,90
16,09	-11,06	15,50	15,60	15,30	15,15	83,89	95,15
16,09	-15,32	15,45	15,45	15,30	14,95	96,88	107,95
16,09	-18,05	15,40	15,30	15,25	14,95	104,28	116,70

Nr. 213: 1,3 % Freon 134 a			dQ_E/dT_B = -2,553; $Q_E(T_B=0)$ = 174,9				
Tp_E °C	Tp_B °C	Tp_1 °C	Tp_2 °C	Tp_3 °C	Tp_4 °C	Q_E W/m²	U_B mV
16,09	14,77	16,10	16,10	16,10	16,30	0,00	0,75
16,09	0,65	15,90	15,75	15,60	15,30	31,33	59,95
16,09	-6,97	15,70	15,60	15,30	14,95	45,21	85,60
16,09	-10,64	15,65	15,60	15,25	14,70	53,22	98,10
16,09	-14,89	15,55	15,40	15,10	14,40	61,89	111,50
16,09	-17,75	15,45	15,35	15,00	14,30	67,21	120,75

Bibliography

1. **Schnell, Michael.** Experimentelle Verifikation des Treibhauseffektes Teil 1: Die gegenseitige Beeinflussung von Wolken und Treibhausgasen. [Online] 25. März 2018. https://www.eike-klima-energie.eu/2018/03/25/experimentelle-verifikation-des-treibhauseffektes-teil-1-die-gegenseitige-beeinflussung-von-wolken-und-treibhausgasen/.

2. **Schönwiese, Christian-Dietrich.** *Klimatologie.* Stuttgart : Eugen Ulmer GmbH, 1994.

3. **Wagner, Thomas.** Strahlungsprozesse in der Atmosphäre. [Online] [Zitat vom: 28. Mai 2018.] https://www.mpic.de/fileadmin/user_upload/pdf/Physik_der_Atmosphaere_Lecture_Wagner.pdf.

4. **Michael Krueger.** Das Pyrgeometer von Knut Angström und die Bestimmung der Gegenstrahlung des atmosphärischen „Treibhauseffekts. [Online] 8. Oktober 2014. http://www.science-skeptical.de/blog/das-pyrgeometer-von-knut-angstroem-und-die-bestimmung-der-gegenstrahlung-des-atmosphaerischen-treibhauseffekts/0012776/.

5. **Albrecht, Fritz.** *Untersuchungen über den Wärmehaushalt der Erdoberßäche in verschiedenen Klimagebieten.* Reichsamt für Wetterdient. Berlin : Julius Springer, 1940.

6. **F. Sauberer.** Registrierungen der nächtlichen Ausstrahlung. *Archiv für Meteorologie, Geophysik und Bioklimatologie, Serie B.* 1951, Bde. Vol. 2, Seiten 347-359.

7. **Möller, Fritz.** *Einführung in die Meteorologie.* Mannheim/Wien/Zürich : Bibliographisches Institut, 1973. Bd. II.

8. Atmosphärische Gegenstrahlung. [Online] 17. April 2017. [Zitat vom: 1. Mai 2017.] https://de.wikipedia.org/..

9. **Ewald Zmarsly, Wilhelm Kuttler, Hermann Pethe.** *Meteorologisch-klimatologisches Grundwissen: Eine Einführung mit Übungen, Aufgaben und Lösungen.* Stuttgart : Eugen Ulmer GmbH & Co., 2002. S. 142.

10. Wolke. [Online] 13. Januar 2006. [Zitat vom: 01. Mai 2018.] https://de.wikipedia.org/wiki/Wolke.

11. **Geiger, Rudolf.** *Das Klima der bodennahen Luftschicht.* Braunschweig : Friedr. Vieweg & Sohn, 1942. S. 64.

12. **Otto Wilhelm Kessler, Wolfgang Kaempfert.** *Die Frostschadenverhütung.* Berlin Heidelberg : Springer-Verlag, 1940. S. 37.

13. **Lönnqvist, Olov.** A window radiation chart for estimating surface temperature from satellite observations. [Online] 19. Oktober 1963. https://www.tandfonline.com/doi/pdf/10.3402/tellusa.v15i4.8856.

14. **LORENZ, DIETER.** Der Einflus einer Luftzwischenschicht auf meteorologische 0berflächentemperaturmessungen mit Radiometern. [Online] 22. Januar 1968. https://onlinelibrary.wiley.com/doi/pdf/10.1111/j.2153-3490.1969.tb00419.x.

15. **Schulze, Rudolf.** *Strahlenklima der Erde.* Darmstadt : Dr. Dietrich Steinkopff, 1970. S. 103. Bd. 72.

16. **Winter, Maiken.** Welche Rolle hat der Wasserdampf beim Treibhauseffekt? [Online] 01. Januar 2008. [Zitat vom: 24. Mai 2018.] https://www.cleanenergy-project.de/gesellschaft/green-lifestyle/wasserdampf-treibende-kraft-beim-treibhauseffekt/.

17. **Christopher J. Cox, Penny M. Rowe, Steven P. Neshyba, and Von P. Walden.** A synthetic data set of high-spectral-resolution infrared spectra for the Arctic atmosphere. [Online] Earth Syst. Sci. Data, 8, 199–211, 2016, 18. 01 2016. [Zitat vom: 23. 01 2018.] https://www.earth-syst-sci-data.net/8/199/2016/essd-8-199-2016.pdf.